JOURNAL OF MASS SPECTROMETRY
J. Mass Spectrom. 2007; **42**: 178–186
Published online 18 December 2006 in Wiley InterScience
(www.interscience.wiley.com) DOI: 10.1002/jms.1148

JMS

Isomeric identification by laser control mass spectrometry

Johanna M. Dela Cruz,[1] Vadim V. Lozovoy[1] and Marcos Dantus[1,2]*

[1] Department of Chemistry, Michigan State University, East Lansing, MI 48824, USA
[2] Department of Physics and Astronomy, Michigan State University, East Lansing, MI 48824, USA

Received 10 August 2006; Accepted 25 October 2006

The influence shaped femtosecond laser pulses have on molecular photofragmentation and ionization, coupled with the intrinsic sensitivity of mass spectrometry, results in a powerful tool for fast, accurate, reproducible and quantitative isomeric identification. Complex phase functions are introduced to enhance differences during the laser–molecule interactions, which depend on geometric structure, resulting in different fragmentation fingerprints. A full account is given on the setup and results leading to a technique that can be used to distinguish between compounds normally indistinguishable by conventional electron ionization mass spectrometry. We demonstrate geometric and structural isomer identification of *cis*-/*trans*-3-heptene, *cis*-/*trans*-4-methyl-2-pentene, *o*-/*p*-cresol and *o*-/*p*-xylene. For the positional isomers of xylene we present a complete dataset consisting of 1024 different phases to explore phase complexity. A selection of two phases from that data can then be used to achieve quantitative identification in mixtures of xylene isomers. Finally, we evaluate receiver operational curves obtained from our experimental data to demonstrate the reliability that can be achieved by femtosecond laser control mass spectrometry. Copyright © 2006 John Wiley & Sons, Ltd.

KEYWORDS: pulse shaping; coherent control; adaptive control; metabolomics; proteomics

INTRODUCTION

Mass spectrometry (MS) has developed rapidly from being a research tool used primarily in physical organic chemistry to the point where biochemical and medical research applications not only account for a high proportion of its usage but also direct much of the effort concerned with technique development. Recent major developments have increased and continue to expand its scope of application in medical research and other areas. These include the effective use of high mass spectrometric sensitivity and the development of techniques for the analysis of compounds of high mass and low volatility which were previously impossible to analyze. Beyond compositional information, structural information is extremely important because different isomers can have widely varying toxicological properties and environmental impacts. Molecular recognition requires a combination of high sensitivity and spectroscopic acuity. Femtosecond pulse shaping technology provides a new dimension to presently used MS approaches, aimed at providing structure selective fragmentation that can be used to greatly enhance molecular recognition.

In most standard implementations of MS, fragmented mass spectra are typically obtained from the energetic ionization process involving collision between neutral analyte molecules and electrons that are typically accelerated to energies between 50 and 150 eV. For most organic compounds, electron ionization (EI) has its highest cross section in the region of 70 eV, where enough excess energy is transferred to the molecule to generate fragmentation of the ion. Such fragmentation can be very useful in providing structural information. For this reason, there exist extensive libraries of mass spectral data at the standard ionization condition of 70 eV EI. (In most 70 eV EI experiments, approximately 1400 kJ/mole (15 eV) of energy is transferred during the ionization process. There is, however, a distribution of energy, and as much as 2800 kJ/mole (30 eV) is transferred to some molecules. Since approximately 960 kJ/mole (10 eV) is required to ionize most organic compounds and a typical chemical bond energy is 290 kJ/mole (3 eV), extensive fragmentation is often observed in 70 eV EI mass spectra.) There are, however, disadvantages to this approach. First, the analysis can become very difficult in the case of complex mixtures. Moreover, it is often the case that different species of the same basic molecular type yield practically identical fragmentation patterns. For example, isomeric compounds yield virtually indistinguishable mass spectra.

The ability of spectroscopic analytical methods such as infrared, Raman and nuclear magnetic resonance spectroscopy to distinguish between pairs or sets of isomers is indisputable. Nevertheless, the orders of magnitude lower detection limit of MS, with the possibility for achieving single ion sensitivity, should give MS an added advantage over these methods. Another significant asset of MS is its

*Correspondence to: Marcos Dantus, Chemistry Building, Michigan State University, East Lansing MI 48824, USA.
E-mail: dantus@msu.edu

capability of handling complex mixtures in tandem with GC.[1]

Although GC/MS is widely used for a variety of environmental, biological and other applications, the interpretation of the resulting data can be complex and time consuming.[2] While many laboratories have such instrumentation, its use for isomeric identification is not trivial. Significant time and effort must be put into selecting the best column for the particular compounds in question; standards must be prepared for each target compound; and the GC temperature program must be optimized to provide efficient separation of compounds. The response function must be determined from the analysis of the standards. The entire process is prone to numerous pitfalls such as contamination, carryover and misinterpretation of the data.

Various MS techniques have been developed to distinguish among different molecular isomers. Isomeric differentiation has been achieved by combining GC, selective self-ion/molecule reactions and tandem MS in ion trap mass spectrometers, but the whole process takes several minutes.[3,4] Isomeric compounds of pentane have, for instance, been distinguished by monitoring the products of their reactions with mass-selected ions generated from the individual isomers in an ion trap.[5] Resonance-enhanced multiphoton ionization employing molecular cooling in a supersonic beam has also been used to separate isomers, although a tunable UV laser source and a special coupling of a GC column and a supersonic beam valve are necessary.[6] Chemical reactivity has been coupled with MS for identification,[7,8] though this wet-chemistry approach is time consuming and its universality uncertain. Certain isomers have been differentiated by electrospray ionization (ESI) tandem MS.[9] Capillary electrophoresis combined with ESI-MS has been applied to the analysis of polar positional and geometrical anionic isomers using a bare fused silica capillary and volatile ammonium acetate buffer.[10] The use of single-drop microextraction in addition to GC/MS is a promising methodology, although the microextraction process requires careful optimization of a number of parameters including the extraction solvent, rate of sample agitation, extraction time, ionic strength of the sample solution and extraction temperature.[11] The two-dimensional separation capability of ion mobility spectrometry (IMS)/MS demonstrated the capability for identification and separation of metabolic isomers within 70 s. High-performance liquid chromatography (HPLC) in conjunction with atmospheric pressure chemical ionization (APCI) MS (HPLC/APCI-MS) enabled the positional isomers of individual triacylglycerols in mixtures to be identified.[12] Several other MS methods combined with a variety of separation procedures have been demonstrated by a number of research groups; however, this is the first time, to our knowledge, that shaped femtosecond laser pulses are demonstrated to provide a new dimension to MS, which allows sub-second identification and quantification of a number of isomeric organic compounds.

Femtosecond lasers have long been used as a source of ions in MS; in most cases these studies were aimed at measuring ultrafast photodissociation dynamics.[13,14] The energy deposited by the laser pulse on the molecules sets off a number of competing processes, primarily ionization, redistribution of energy among the different degrees of freedom in the molecules and fragmentation. It has recently been shown that the relative yield of the resulting fragment ions can be controlled to some extent by shaping the femtosecond laser pulses.[15] Specific phase functions that determine the relative phase of different frequency components in the pulse can be introduced using a pulse shaper.[16] At present, there is no theoretical model that provides a link between pulse shaping and its effects on molecular ionization and fragmentation. While such a model is still to be developed, empirical searches guided by computer learning algorithms, as suggested by Judson and Rabitz,[17] had been used to explore the extent of selectivity.[14,18,19]

The Dantus group has developed a method that extensively evaluates an entire subset of phase functions in a few minutes while introducing a varying degree of multiphoton intrapulse interference[20,21] occurring among excitation pathways during laser-induced ionization and fragmentation. The search for the optimal phase function is expedited and made more efficient by considering only binary phase functions,[22] where the relative phase between different frequencies is either 0 or π, and only a small number of frequency regions (pixels) are modified. The sensitivity of laser–molecule interactions to differences in electronic and molecular structures of compounds is amplified by binary phase modulation.[23] As few as 8-bit binary phase functions have been shown to be capable of changing the relative yield of particular fragments by 2 orders of magnitude. Once appropriate binary phases are selected, isomeric molecules can be identified, and quantitative assessment of their relative concentration in isomeric mixtures is possible on a sub-second timescale.

We reported elsewhere a brief account on using shaped laser pulses to control the ionization and fragmentation of isomeric molecules to accomplish isomer identification.[24] Here we elaborate on the methodology involved and test it for the identification of the structural isomers of cresol (*ortho* and *para*) and the geometric (*cis, trans*) isomers of 3-heptene and 4-methyl-2-pentene (MP). The core of this study corresponds to the data obtained for *o- and p*-xylene. The xylene isomers are of great importance to the petrochemical industry because they are precursors in the synthesis of many organic compounds.

EXPERIMENTAL

The laser system used for this study is a commercial regeneratively amplified titanium : sapphire femtosecond laser with an output of 0.8 mJ/pulse centered at 800 nm with 1 kHz repetition rate. The laser has been configured with a pulse shaper between the oscillator and the amplifier, which uses the multiphoton intrapulse interference phase scan (MIIPS) method[25–27] to obtain 35 fs transform-limited (TL) pulses or to introduce specific binary phase functions. This pulse shaping technology was licensed to BioPhotonic Solutions Inc. and is commercially available from Coherent Inc. in their Silhouette pulse shaper. The correction of phase distortions to generate TL pulses is critical for

JMS

experimental precision and reproducibility because the nonlinear interaction between the laser pulses and the molecules is very sensitive to phase variations in the laser pulse. It is this nonlinear interaction that leads to ionization and fragmentation. For most organic compounds, about six photons (~9 eV) of light with wavelength centered at 800 nm are necessary to bring about ionization. To ensure repeatability, the second harmonic generation (SHG) spectrum of the laser is recorded for every phase function tested. The SHG spectrum provides an accurate diagnostic of the laser pulses.

Binary phase functions are introduced at the Fourier plane of the pulse shaper, where the spectrum of the pulse is fully dispersed. Each phase function contains ten groups of ten pixels. A phase retardation equal to 0 or π is assigned to the ten corresponding regions in the spectrum of the pulse. Because only the phase of the pulse is modulated, the energy and the spectrum of the excitation laser field stay unaltered throughout the experiment. The phase-shaped laser pulses are then focused inside a low-pressure gas chamber where they interact with the gaseous sample molecules causing ionization and fragmentation.

The experimental data were obtained using a vacuum system equipped with a time-of-flight (TOF) mass spectrometer. The samples included the *ortho* and *para* isomers of xylene and cresol, and the *cis/trans* isomers of the alkenes 3-heptene and MP (Sigma Aldrich). These compounds were used without further purification. The sample vapor was allowed to leak into the TOF chamber until the pressure increased to about 1×10^{-5} Torr (for the xylene and cresol isomers) or about 8×10^{-6} Torr (for the geometric isomers). The chamber was continually pumped by a 220 l/s turbomolecular vacuum pump, where the fast flow prevented the accumulation of fragments. The ions were allowed to travel in a drift-free zone of about 0.5 m before being detected by a microchannel plate. The system has a mass resolution of 1000. Each mass spectrum obtained represents the signal average resulting from 128 laser shots. The laser was attenuated to 130 μJ/pulse at the TOF chamber entrance. The setup for the experiment is shown in Fig. 1. Recently we confirmed that phase modulation introduced by Shaper I is very accurate implying there is no need for Shaper II.

A total of 1024 different binary phases representing all possible 10-bit binary phase functions were evaluated. The binary phases are referred to in the text as BP*X*, where *X* corresponds to the decimal value of the binary number; i.e. the phase function 0 000 000 000 corresponds to BP0 and 1 101 011 010 corresponds to BP858, where 1 is replaced by π retardation at the corresponding position in the spectrum. Each electric field is allowed to interact with the system and a measure of the effect of each shaped laser pulse is collected. The ratios or differences of peak integrals representing different fragmentation channels are typically used to evaluate the suitability of each laser pulse that produces a TOF-MS. Some binary phase functions cause large enough differences in the fragmentation and ionization patterns that can be used to identify isomers and even quantify their concentration in a mixture.

RESULTS

For some isomer pairs, the standard 70-eV EI-MS shows sufficient differences in terms of relative abundances of the molecular ion and its fragments so that identification might be possible. Among the compounds tested by us, the maximum differences ranged from 2 to 30%. Given a typical uncertainty of as much as 10% in EI-MS, most isomer pairs, for example, the xylene pair analyzed in detail here, are virtually indistinguishable. Figure 2 shows the differences in relative abundances of each fragment ion between the pairs of isomers studied. The plots shown were derived from standard National Institute of Standards and Technology (NIST) data[28] and were obtained by subtracting the 70-eV EI-MS of one compound from that of its isomer. Before these difference spectra were obtained, all peaks in the original mass spectra were normalized to the highest mass ion peak for each isomeric sample. The statistical reliability of the mass spectral data used, specifically in terms of the peak intensities, was not provided. The <3% difference in fragment-ion abundances between the *ortho* and *para* isomers of xylene is depicted in Fig. 3. The mass spectra obtained

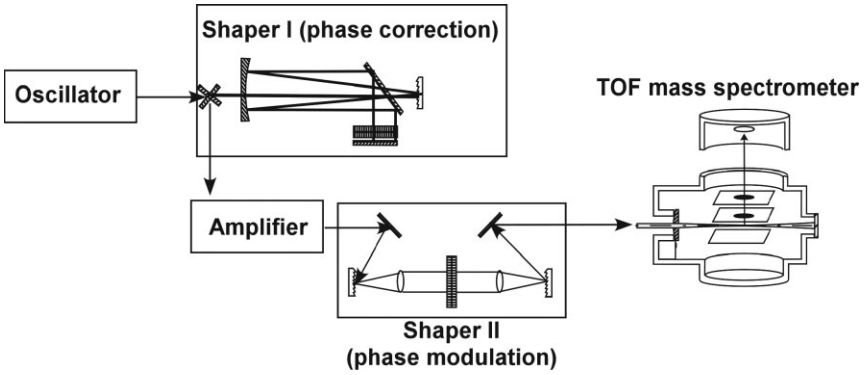

Figure 1. Experimental setup. The beam from the oscillator goes through a pulse shaper, where spectral phase distortions of the pulse are measured and corrected before being amplified. The amplified pulses then go through a second pulse shaper where the spectral phase is modulated. The shaped pulses then enter a TOF-MS chamber where they interact with the sample. Ionization and fragmentation of the sample molecules are then detected by a microchannel plate detector coupled to an Infinium 54 830 digital oscilloscope.

DOI: 10.1002/jms

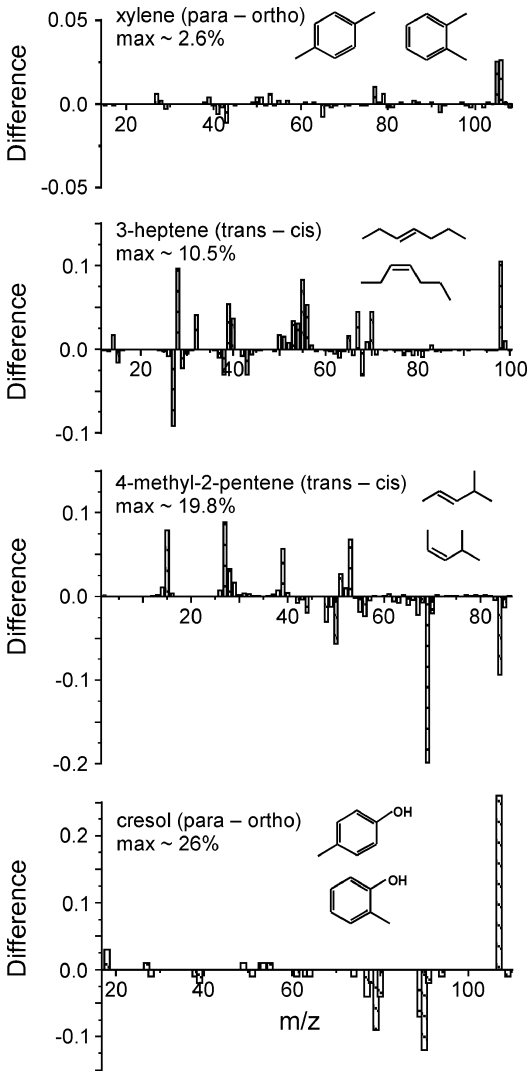

Figure 2. Difference mass spectra of the various sample isomeric pairs tested: xyelene, 3-heptene, 4-methyl-2-pentene (MP) and cresol. The structures of the compounds are also shown.

from EI (70 eV) clearly show negligible differences between the xylene isomers.

Since the error associated with the intensity of a single fragment-ion peak can sometimes be unpredictable, analysis of data obtained with the femtosecond laser was focused on deciphering mass spectral differences of isomeric pairs of molecules based on ratios of intensities between two fragment-ion peaks. Such peaks were chosen on the basis of the maximum ion ratio differences obtained between the isomers. The experimental mass spectra obtained for the xylene isomers were analyzed on the basis of the ratio between the peak value obtained for the molecular ion (M^+, $m/z = 106$) and the tropylium ion[29] (T^+, $m/z = 91$).

The role of phase complexity is explored in Fig. 4, where the ion ratios (m/z 91/106) are given for *ortho*- (open squares) and *para*- (black circles) xylene for all 1024 different binary phases. When sorted, phase functions are grouped to provide a statistical indication of phase complexity. The ion ratios

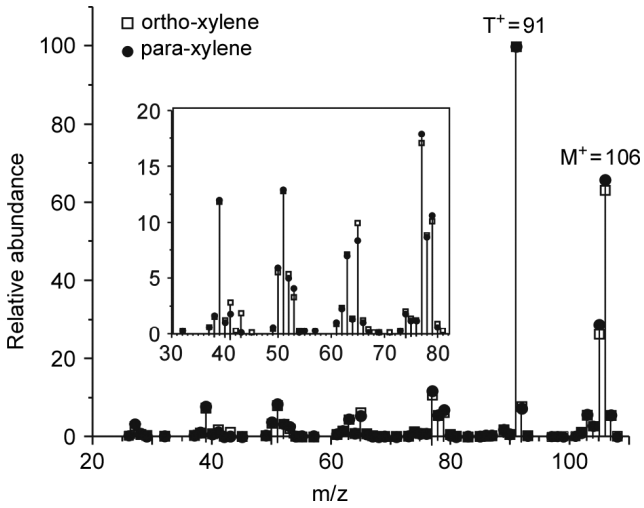

Figure 3. Electron ionization (NIST) mass spectra obtained for *o*-(open squares) and *p*-xylene (filled circles). The inset shows the same on a reduced scale.

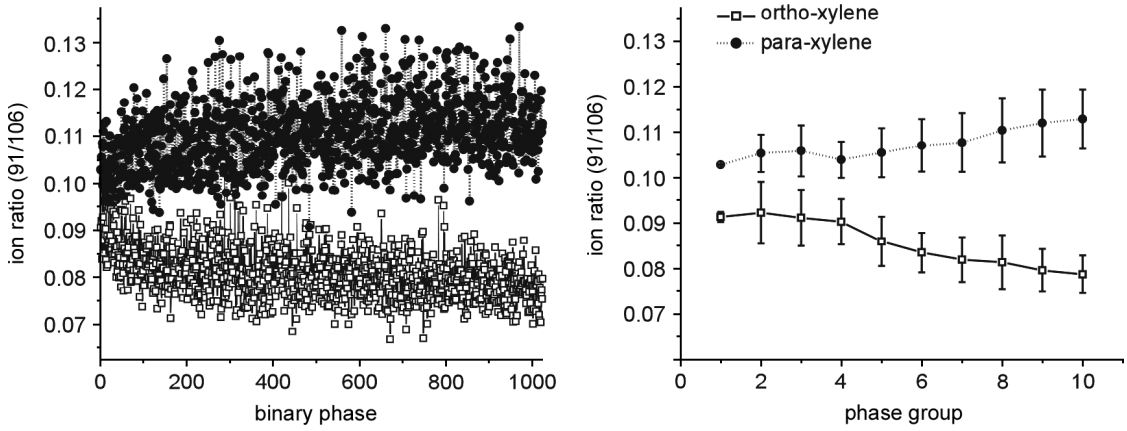

Figure 4. Left: Correlation of ion ratio intensity (m/z 91/106) and sorted phase function for *o*- and *p*-xylene. *o*-Xylene is clearly distinguishable from *p*-xylene. The difference is observable for most of the phase functions used. Right: Grouping the sorted binary phases according to complexity shows maximum contrast (m/z 91/106) between the isomers for more complex phase structures. Phase group 1 consists of two binary phases, group 2 contains 4, group 3 has 8, group 4 has 16, group 5 has 32, group 6 has 64, group 7 has 128, group 8 has 256, group 9 has 256 and group 10 consists of 258 binary phase functions. The binary phases were sorted on the basis of their effect on SHG intensity.

JMS

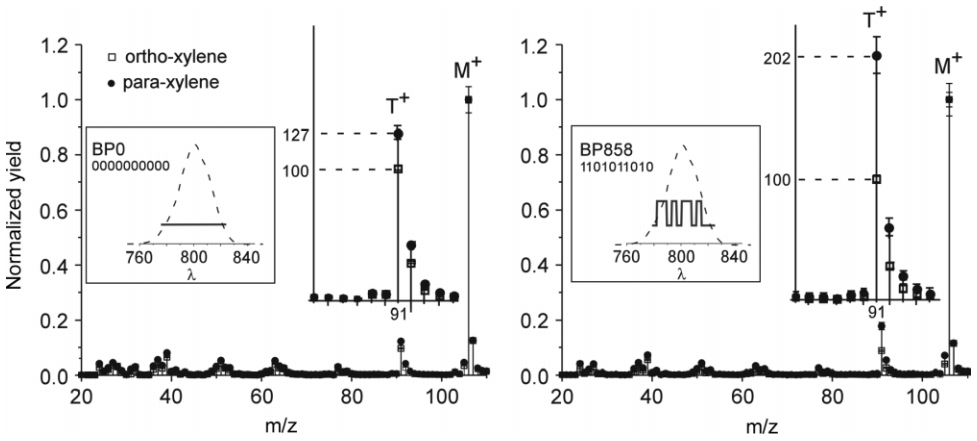

Figure 5. Mass spectra of the xylene isomers. Left: Results obtained with BP0 corresponding to TL laser pulses; the spectral phase of the laser pulse is shown above the mass spectra. Right: Data obtained with laser pulses with binary phase BP858; the phase structure of this pulse is shown above the mass spectra of the isomers. All mass spectra were normalized so that the molecular ion (M^+) intensity equals unity. The region for *m/z* near 91, corresponding to the tropylium ion (T^+), was amplified to highlight the observed differences. For the BP858 shaped pulses, the relative yield of T^+ for *p*-xylene is ~2 times greater than that observed for *o*-xylene.

obtained clearly distinguish one isomer from the other (Fig. 4, right)

Figure 5 shows the mass spectra obtained from femtosecond laser excitation (flat phase to a more complicated binary phase function) of the vaporized isomeric samples. A flat phase function produces TL pulses, which are designated here as BP0. Such pulses already point to small, yet identifiable differences between *o*- and *p*-xylene. The application of a complex binary phase-shaped pulse resembling BP858 results in a much greater relative yield of the tropylium ion for *p*-xylene compared to that of *o*-xylene. The mass spectral fingerprints were normalized to the molecular ion peak. The fragment-ion peak at m/z 91, which in EI-MS is the most dominant peak, decreases in abundance when the laser is used as the excitation source. The differences observed for the other major fragment ions were not as significant, and were not further analyzed.

Figure 6 shows the statistical distribution of the ratios between the molecular ion and the tropylium ion obtained for each isomer, highlighting the contrast achieved using binary shaped pulses. The ratios are represented by histograms of 100 independent measurements for each sample and for each phase. For TL pulses, a slight difference between the two isomers is apparent. However, this difference is enhanced when the binary phase BP858 is used to ionize and fragment the xylene isomers.

The ratio between ionic fragments at m/z 106 and 91 (106/91) for *o*-xylene (11.21 ± 0.40) is about a factor of 2 greater than *p*-xylene (5.62 ± 0.17). When compared to TL pulses, the shaped pulse improved fragmentation, leading to a lower M^+/T^+ ratio for *p*-xylene. Interestingly, the opposite trend was observed for *o*-xylene. TL pulses also gave relatively greater ion ratios for *o*-xylene (10.53 ± 0.17) than for *p*-xylene (8.18 ± 0.14), but the difference between the isomeric ratios is less.

The quantitative performance of our method was assessed by the analysis of six different mixtures of the

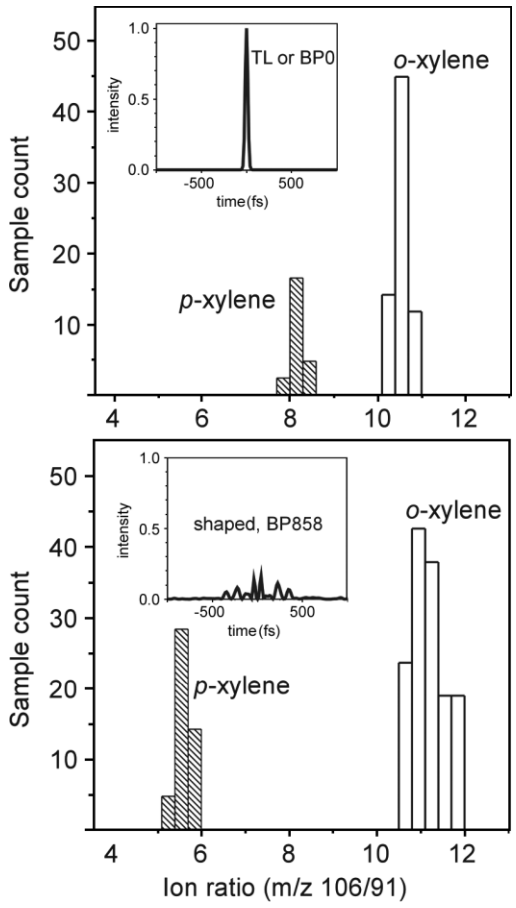

Figure 6. Histograms depicting the statistical distribution of the experimentally measured ratio (M^+/T^+) obtained for 100 independent measurements each for *o*- and *p*-xylene. Top: Histograms obtained using laser pulses with phase BP0; the inset shows the time structure of the pulse. Bottom: Histograms obtained using laser pulses with phase BP858; the inset shows the time structure of the pulse. The histograms obtained for BP858 show a greater molecular-ion-to-tropylium-ion ratio. The observed differences can be used for fast and reliable identification between these two isomers.

DOI: 10.1002/jms

two xylene isomers. The mixtures were probed by the phase-shaped pulses, and the ratio of the molecular ion to tropylium ion peaks for each mixture was recorded. Data for two independent sets of measurements plotted as a function of concentration are shown in Fig. 7. The linear behavior of the data agrees with the analytical formula:

$$\left(\frac{M^+}{T^+}\right)_{\text{normalized}} = \left[\frac{(M^+/T^+)_{\text{experimental}} - (M^+/T^+)_0}{(M^+/T^+)_1 - (M^+/T^+)_0}\right] \quad (1)$$

where $(M^+/T^+)_{\text{experimental}}$ is the measured peak ratio for each sample mixture. $(M^+/T^+)_0$ is the peak ratio measured for a pure *p*-xylene sample, and $(M^+/T^+)_1$ is the measured peak ratio for pure *o*-xylene. The normalized molecular-ion-to-tropylium-ion ratios directly provide the relative concentration of the *ortho* isomer in the mixture. Small differences in total ion intensities of the samples when TL pulses were used were accounted for by normalization of the collected data.

Simplified experimental mass spectra obtained for the isomeric pairs of 3-heptene, MP and cresol are shown in Fig. 8. The fingerprints for each isomeric pair were obtained using different binary phase-shaped pulses. The spectra show selected major fragment-ion peaks for each isomeric pair, normalized to the molecular ion peak of each compound. Ratios between the selected peaks for each of the isomers were maximum for the indicated mass spectra. Although minor peaks provided sizable ion ratios, their usefulness for quantitative work is diminished by their greater susceptibility to noise.

The maximum ratio difference observed for xylene in particular corresponds to a difference of roughly 50%, which, when compared to the NIST difference (~3–4%) (Fig. 2), makes an amazingly straightforward distinction between

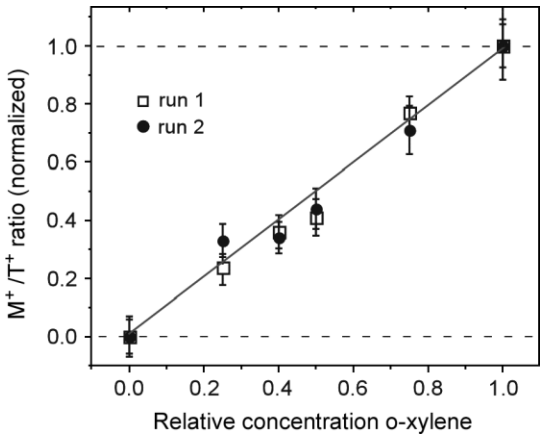

Figure 7. Quantitative concentration measurements of isomeric mixtures using laser control MS. Each data point represents an average of 100 measurements (0.1 s total) obtained for each of six different mixtures. The horizontal axis corresponds to the known concentration of each of the mixtures. The vertical axis corresponds to the normalized M^+/T^+ ratio, which increases linearly with the relative concentration of *o*-xylene. This linear relationship provides a quantitative method to determine the concentration of each of the isomers (*o*- and *p*-xylene) in a mixture. Two sets of data obtained on two different days are shown to illustrate the robustness of this method.

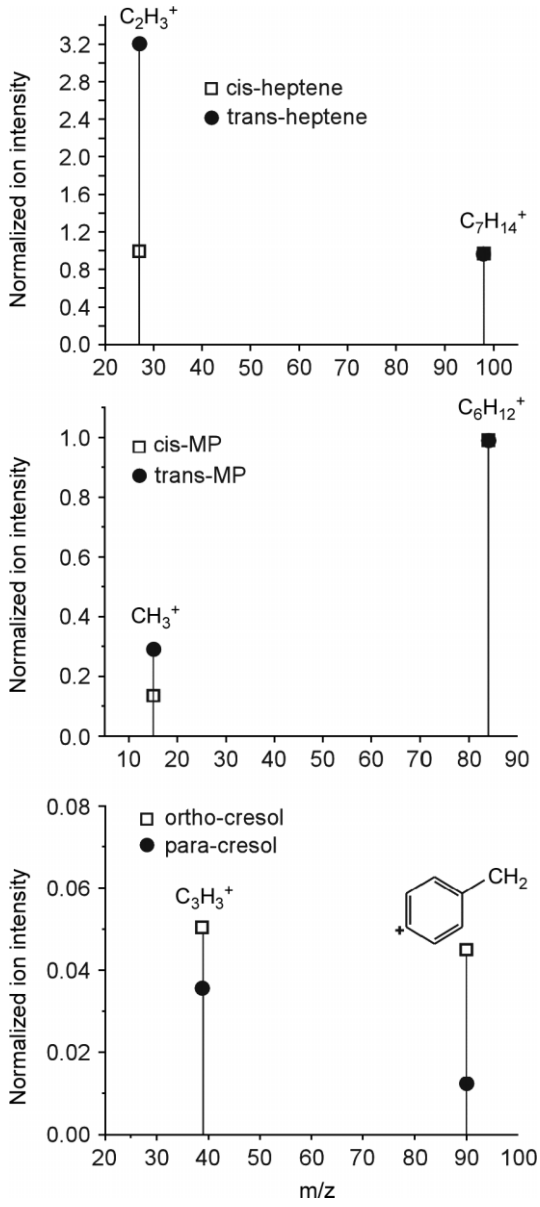

Figure 8. Mass spectra obtained for the isomeric pairs of 3-heptene, MP and cresol using binary shaped pulses. The fingerprints show only the *m/z* values for each isomer where ratios were maximum for a given binary phase.

the two isomers. Although the rest of the isomers already showed disparities in their NIST spectra, these differences were enhanced several times more with shaped femtosecond laser irradiation.

DISCUSSION

Shaped femtosecond laser pulses are shown here to be a flexible tool to control molecular fragmentation and ionization and can be used to identify between isomeric pairs of molecules. As a consequence of multiphoton absorption, the fragmentation of molecules can be attained by either of two distinct mechanisms – the process of dissociation followed by ionization (DI, ladder switching) or ionization followed by dissociation (ID, ladder climbing).[30,31] On the basis of the mass spectra obtained and because of the

JMS

short pulse duration of the laser,[31] the xylene molecules fragment by the ID route: the molecules absorb a number of photons to reach a dissociative state below the ionization level. If the laser pulse length is longer than the lifetime of the state, then the molecular fragments form neutral moieties. Depending on the laser intensity, these fragments may absorb additional photons within the initial laser pulse to ionize or further fragment. For xylene and most organic compounds, ionization energies range from 8 to 9 eV. The absorption of six photons of energy $h\nu$ of 1.55 eV each should be sufficient to induce ionization. As shown by measurements of photoelectron energies,[32] molecules ionize as soon as the sum of absorbed photon energies exceeds the lowest ionization potential. Subsequent absorption by the ion results in extensive fragmentation.[33–36] An observed power dependence of the ion peaks confirms that molecular fragmentation of xylene follows the ID mechanism, as suggested by Kosmidis *et al*. in their study of the nitrotoluene isomers.[37]

It is interesting to understand the mechanism responsible for the observed laser-based recognition. The nonlinear optical polarizability of molecules is highly dependent on molecular structure.[38] Strong laser fields have been found to cause charge buildup at the ends of extended conjugated systems, resulting in ionization by tunneling or barrier suppression.[39] A greater nonlinear optical polarizability increases a molecule's susceptibility to undergo fragmentation. This is consistent with our results for xylene, and with the slightly lower ionization energy of *p*-xylene (8.44 ± 0.05 eV) compared to that of *o*-xylene (8.56 ± 0.04 eV). This observation was also evident in the other isomeric samples, where the structures of *trans*-3-heptene and *trans*-MP make them more polarizable than their isomeric partners. Consequently, the yield of most of their ion peaks is relatively greater than those of their isomeric counterparts.

The complexity of the structures of the binary phase functions that provided maximum contrast between isomeric pairs largely affected the responses of the molecules. The temporal profiles for the different laser pulses used here are quite diverse, as represented by TL (or BP0) and BP 858 laser pulses (Fig. 6). The observed outcome of the reaction could be attributed to the time–frequency structure of the pulse. Although the total ion yield was about 6 times lower for shaped pulses than for TL pulses, the differences observed between the isomers appear to have increased with pulse shaping. A direct link between the binary phase modulation of the pulse and the selective molecular response has yet to be established; however, the observed differences allowed us to devise a quantitative measurement of the relative concentration in a mixture of these isomers.

The quantification of molecules in mixtures can also be demonstrated through the use of receiver operation characteristic (ROC) curves.[40] An ROC curve is a graphical representation of the trade-off between the true-positive and false-positive rates for every possible cutoff. Equivalently, it represents the trade-offs between sensitivity (true positive) and specificity (false-positive: 1 – specificity) classifications resulting from each possible decision threshold value. A measurement is considered positive if the value is above some arbitrary cutoff, and is negative if it is below the cutoff. When applied to the quantification of xylene isomers, for instance, it provides an estimate of the probability for positive (or negative) identification of an isomer in a given mixture. The probability of a correct isomeric identification drops to 50% when the ROC curve overlaps the cutoff level, i.e. a rising diagonal or chance line. On the contrary, when this probability increases, the area under the ROC curve is higher and the curve tends to approach the left-hand corner, corresponding to the highest theoretical value of accuracy. The scenario in which ROC curves are used to plot differences between two isomers is depicted in Fig. 9. The left panel demonstrates good contrast between two isomers. The true-positive rate, which, in this case represents the probability of the presence of *p*-xylene, is high and the false-positive rate (*o*-xylene) is low. The middle and right panels show cases where the probability of correct identification decreases. Generally, the points where overlap between histograms of data occur (top portions of figure) are less likely to provide better discrimination. A perfect

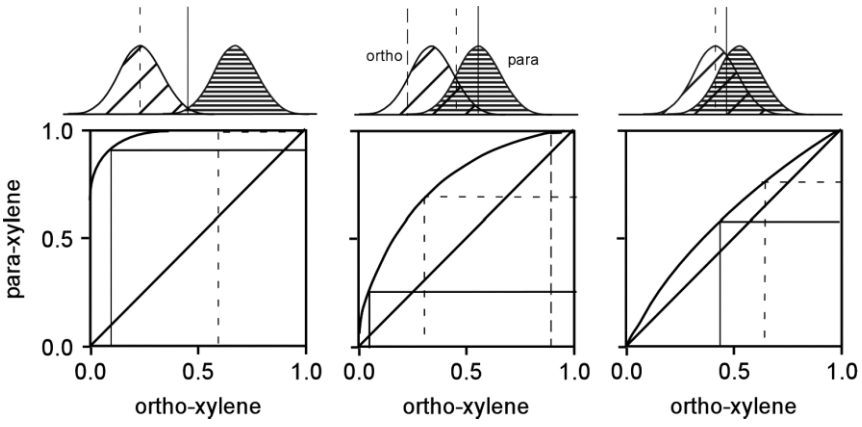

Figure 9. Schematic ROC curves for isomeric distinction. When the statistical measurements for *o*-xylene are well separated from those of *p*-xylene, the ROC curve is almost flat, indicating increased accuracy in the discrimination between the isomers. When the overlap is greater, the ROC curve tends to move closer toward the chance line (diagonal line from the bottom left corner to the upper right corner). When the curves overlap almost totally, the ROC curve turns into the chance line.

DOI: 10.1002/jms

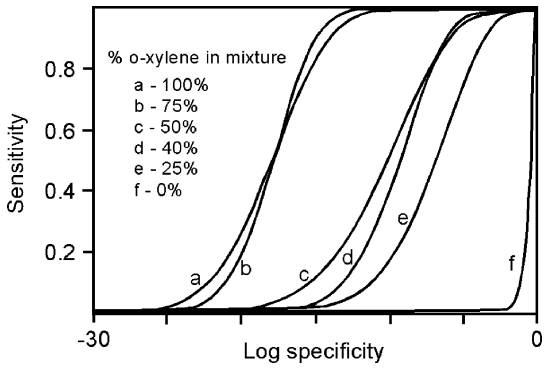

Figure 10. Experimental ROC curves representing the relative concentrations of *o*-xylene in variable mixtures of *o*- and *p*-xylene. Each curve, labeled (a), (b), (c), (d), (e) and (f), corresponds to the amount (in percentage) of *o*-xylene in the mixture. Note the logarithmic specificity axis.

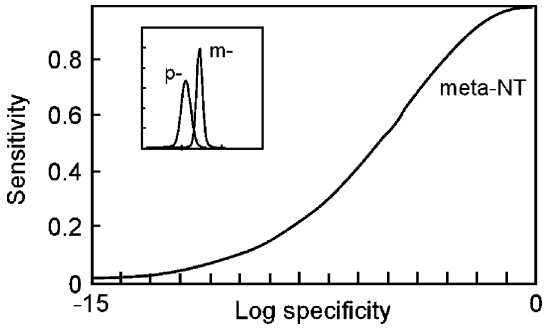

Figure 11. Estimation of probable contrast ratios between isomeric mixtures. ROC curve prediction based on experimental data obtained from pure *meta*- and pure *para*-nitrotoluene samples. The curve was calculated for *m*-nitrotoluene in a 1 : 1 mixture with its *p*-isomer. The inset shows the calculated Gaussian distribution for the defined mixture. Note the logarithmic specificity axis.

identification test would have 100% sensitivity and 100% specificity.

Figure 10 shows the ROC curve derived from the experimental data shown in Fig. 7. The illustration shows the use of ROC curves for the discrimination between the relative concentrations of *o*-xylene in different mixtures. By tradition, ROC curves show the false-positive rate (1−specificity) on the *x*-axis and true-positive rate (sensitivity) on the *y*-axis. The data represent an almost ideal scenario in which all curves climb rapidly toward the upper left-hand corner of the graph and positive identification is very likely. In other words, the accuracy of the data in terms of predicting quantitative measurements is reasonably high. The plot shown in Fig. 10 is a modification of the traditional ROC curve, wherein the logarithmic value of the specificity is plotted on the *x*-axis. This was done to better visualize the differences between curves representing the various isomeric concentrations in a mixture.

Similarly, ROC curves can be used to estimate the probable concentration of a mixture of isomers on the basis of experimental mass spectral data from pure isomers. Figure 11 illustrates this case with nitrotoluene (NT), where the ratio between fragment ions at m/z 91 and 39 is obtained for *para*- and *meta*-NT. The ROC curve shows the probability of distinguishing *m*-nitrotoluene from a 1 : 1 mixture of *m*- and *p*-nitrotoluene.

One of the major objectives of our work is the extension of MS to problems in biomedical chemistry. A future research effort is directed toward developing laser control methods for elucidating the structure of peptides and proteins. In metabolomics, the coupling of the high sensitivity of femtosecond laser control with the high resolution of MS could provide a method for determining a rough estimate of the number of metabolites present. MS could offer a valuable first indication of the identities of molecules, while laser control contends with its inability to separate molecules of the same molecular mass. Even as emerging MS technologies continue to cope with the expanding demand for applications in a wide range of areas, the complexity associated with these techniques is a drawback. Controlled fragmentation with femtosecond laser pulses is a viable alternative to most existing hyphenated (e.g. GC-MS, LC-MS, IMS-MS) and tandem MS methods, in terms of its ability to rapidly discriminate between structural isomeric compounds.

CONCLUSIONS

The principle of molecular fragmentation and ionization control by pulse shaping with binary phase functions was used to expand the capabilities of conventional MS to include fast, accurate and reproducible qualitative and quantitative isomeric identification. This approach provides a new dimension in MS that is highly sensitive to molecular structure, as required by current biological and environmental applications. While there are a number of technological platforms available for chemical, including isomeric, identification, none is perfect, with each method providing different merits. Although the perceived notion is that coherent control using femtosecond lasers is too complicated and too expensive to be useful to biologists and environmental scientists, awareness of its potential capabilities for analytical work and its eventual applications in the biomedical field substantiate further investigation of this technology. The commercial availability of one-box 'no-expert-required' femtosecond lasers and laser systems with integrated pulse shapers will facilitate the use of laser control in MS.

Acknowledgements

This research was supported by the National Science Foundation. Partial support to Vadim Lozovoy came from an STTR grant from the Army Research Office to BioPhotonic Solutions, subcontract to MSU, and is gratefully acknowledged. (The content of the information does not necessarily reflect the position or the policy of the Government; no official endorsement should be inferred.)

REFERENCES

1. Burlingame AL, Shackleton CHL, Howe I, Chizhov OS. Mass spectrometry. *Anal. Chem.* 1978; **50**: R346.
2. Bruckner CA, Prazen BJ, Synovec RE. Comprehensive two-dimensional high-speed gas chromatography with chemometric analysis. *Anal. Chem.* 1998; **70**: 2796.
3. Wu HF, Chuan YJ. Isomer differentiation by combining gas chromatography, selective self-ion/molecule reactions and

tandem mass spectrometry in an ion trap mass spectrometer. *Rapid Commun. Mass Spectrom.* 2003; **17**: 1030.
4. Wu HF, Wu WF. Comparing differentiation of xylene isomers by electronic ionization, chemical ionization and self-ion/molecule reactions and the first observation of methyne addition ions for xylene isomers in self-ion/molecule reactions for non-nitrogenated compounds. *Rapid Commun. Mass Spectrom.* 2003; **17**: 2399.
5. Kascheres C, Cooks RG. Isomer distinction by ion/molecule reactions in an ion trap: the case of C_5H_8. *Anal. Chim. Acta* 2002; **215**: 223, DOI:10.1016/S0003-2670(00)85280-0.
6. Zimmermann R, Lerner C, Schramm K, Kettrup A, Boesl U. Three-dimensional trace analysis: combination of gas chromatography, supersonic beam UV spectroscopy and time-of-flight mass spectrometry. *Eur. J. Mass Spectrom.* 1995; **1**: 341.
7. Brodbelt JS, Liou CC, Donovan T. Selective adduct formation by dimethyl ether chemical ionization in a quadrupole ion trap mass spectrometer and a conventional ion source. *Anal. Chem.* 1991; **63**: 1205.
8. Bjarnason A. Xylene isomer mass spectral identification through metal ion chemistry in an FTICR. *Anal. Chem.* 1996; **68**: 3882.
9. Zhang JM, Brodbelt JS. Structural characterization and isomer differentiation of chalcones by electrospray ionization tandem mass spectrometry. *J. Mass Spectrom.* 2003; **38**: 555, ISI:000 183 171 700 011.
10. Nogami C, Sawada H. Positional and geometrical anionic isomer separations by capillary electrophoresis-electrospray ionization-mass spectrometry. *Electrophoresis* 2005; **26**: 1406, ISI:000 228 784 000 015.
11. Liu BM, Malik P, Wu HF. Single-drop microextraction and gas chromatography/mass spectrometric determination of anisaldehyde isomers in human urine and blood serum. *Rapid Commun. Mass Spectrom.* 2004; **18**: 2059, ISI:000 223 872 700 008.
12. Mottram HR, Woodbury SE, Evershed RP. Identification of triacylglycerol positional isomers present in vegetable oils by high performance liquid chromatography atmospheric pressure chemical ionization mass spectrometry. *Rapid Commun. Mass Spectrom.* 1997; **11**: 1240, ISI : A1997XR69700002.
13. Dantus M, Jannsen MHM, Zewail AH. Femtosecond probing of molecular dynamics by mass spectrometry in a molecular beam. *Chem. Phys. Lett.* 1991; **181**: 281.
14. Baumert T, Buhler B, Thalweiser R, Gerber G. Femtosecond spectroscopy of molecular autoionization and fragmentation. *Phys. Rev. Lett.* 1990; **64**: 733.
15. Assion A, Baumert T, Bergt M, Brixner T, Kiefer B, Seyfried V, Strehle M, Gerber G. Control of chemical reactions by feedback-optimized phase-shaped femtosecond laser pulses. *Science* 1998; **282**: 919.
16. Weiner A. Femtosecond pulse shaping using spatial light modulators. *Rev. Sci. Instrum.* 2000; **71**: 1929.
17. Judson RS, Rabitz H. Teaching lasers to control molecules. *Phys. Rev. Lett.* 1992; **68**: 1500.
18. Levis RJ, Menkir GM, Rabitz H. Selective bond dissociation and rearrangement with optimally tailored, strong-field laser pulses. *Science* 2001; **292**: 709.
19. Cardoza D, Baertschy M, Weinacht TC. Understanding learning control of molecular fragmentation. *Chem. Phys. Lett.* 2005; **411**: 311.
20. Walowicz KA, Pastirk I, Lozovoy VV, Dantus M. Multiphoton intrapulse interference. 1. Control of multiphoton processes in condensed phases. *J. Phys. Chem. A* 2002; **106**: 9369.
21. Lozovoy VV, Pastirk I, Walowicz KA, Dantus M. Multiphoton intrapulse interference. II. Control of two- and three-photon laser induced fluorescence with shaped pulses. *J. Chem. Phys.* 2003; **118**: 3187.
22. Comstock M, Lozovoy VV, Pastirk I, Dantus M. Multiphoton intrapulse interference 6; binary phase shaping. *Opt. Express* 2004; **12**: 1061.
23. Pastirk I, Kangas M, Dantus M. Multidimensional analytical method based on binary phase shaping of femtosecond pulses. *J. Phys. Chem. A* 2005; **109**: 2413.
24. Dela Cruz JM, Lozovoy VV, Dantus M. Isomer identification by mass spectrometry with Shaped femtosecond laser excitation. *J. Phys. Chem. A* 2005; **109**: 8447.
25. Dela Cruz JM, Pastirk I, Lozovoy VV, Walowicz KA, Dantus M. Multiphoton intrapulse interference 3: probing microscopic chemical environments. *J. Phys. Chem. A* 2004; **108**: 53.
26. Lozovoy VV, Pastirk I, Dantus M. Multiphoton intrapulse interference. IV. Ultrashort laser pulse spectral phase characterization and compensation. *Opt. Lett.* 2004; **29**: 775.
27. Xu B, Gunn JM, Dela Cruz JM, Lozovoy VV, Dantus M. Quantitative investigation of the MIIPS method for phase measurement and compensation of femtosecond laser pulses. *J. Opt. Soc. Am. B, Opt. Phys.* 2006; **23**: 750.
28. Stein SE. NIST Mass Spectrometry Data Center. In *Mass Spectra*, Linstrom PJ, Mallard WG (ed.). National Institute of Standards and Technology: Gaithersburg, MD, 2005; NIST Standard Reference Database Number 69.
29. Malow M, Penno M, Weitzel KM. The kinetics of methyl loss from ethylbenzene and xylene ions: the tropylium versus benzylium story revisited. *J. Phys. Chem. A* 2003; **107**: 10 625.
30. Gedanken A, Robin MB, Kuebler NA. Nonlinear photochemistry in organic, inorganic and organo-metallic systems. *J. Phys. Chem.* 1982; **86**: 4096.
31. Yang JJ, Gobeli DA, ElSayed MA. Change in the mechanism of laser multiphoton ionization in benzaldehyde by changing the laser pulse width. *J. Phys. Chem.* 1985; **89**: 3426.
32. Meek JT, Jones RK, Reilly JP. Photoelectron energy distribution following uv laser ionization of gas phase benzene. *J. Chem. Phys.* 1980; **73**: 3503.
33. Zandee L, Bernstein RB. Laser ionization-mass spectrometry–extensive fragmentation via resonance-enhanced multiphoton ionization of a molecular benzene beam. *J. Chem. Phys.* 1979; **70**: 2574.
34. Rockwood S, Reilly JP, Hohla K, Kompa KL. UV laser induced molecular multiphoton ionization and fragmentation. *Opt. Commun.* 1979; **28**: 175.
35. Fisanick GJ, Eichelberger TS, Heath BA, Robin MB. Multiphoton ionization mass spectrometry of acetaldehyde. *J. Chem. Phys.* 1980; **72**: 5571.
36. Robin MB. Multiphoton fragmentation and ionization. *Appl. Opt.* 1980; **19**: 3941.
37. Kosmidis C, Ledingham KWD, Kilic HS, McCanny T, Singhal RP, Langley AJ, Shaikh W. On the fragmentation of nitrobenzene and nitrotoluenes induced by a femtosecond laser at 375 nm. *J. Phys. Chem. A* 1997; **101**: 2265.
38. Lezius M, Blanchet V, Ivanov MY, Stolow A. Polyatomic molecules in strong laser fields: nonadiabatic multielectron dynamics. *J. Chem. Phys.* 2002; **117**: 1575.
39. Smith SM, Markevitch AN, Romanov DA, Li XS, Levis RJ, Schlegel HB. Static and dynamic polarizabilities of conjugated molecules and their cations. *J. Phys. Chem. A* 2004; **108**: 11 063.
40. Hanley JA, McNeil BJ. The meaning and use of the area under a Receiver Operating Characteristic (ROC) curve. *Radiology* 1982; **143**: 29.